JOURNAL OF APPLIED ELECTROCHEMISTRY 19 (1989) 281–286

A numerical method of calculating secondary current distributions in electrochemical cells

AKIRA KATAGIRI

College of Liberal Arts, Kyoto University, Sakyo-ku, Kyoto 606, Japan

YOSHINORI MIYAZAKI

Fuel Cell Section, Goverment Industrial Research Institute, Osaka, Ikeda-shi, Osaka 563, Japan

Received 16 August 1988; revised 8 November 1988

A numerical method is proposed based on the analogy between the potential distribution in an electrolytic solution and the temperature distribution in a heat-conducting medium. Thus the equation of non-steady-state heat conduction which contains a hypothetical temperature $v(x, y, t)$ is solved numerically with appropriate boundary conditions. In the steady state the distribution of $v(x, y, t)$ corresponds to the distribution of potential $\phi_s(x, y)$ which satisfies Laplace's equation. The method is useful not only for conventional electrochemical cells but also for complicated systems such as a bipolar electrode for which boundary conditions provide neither the potential nor the current density at the electrode surface.

Nomenclature

a	length of unit cell (see Fig. 1)
b, c, d	geometric parameters of rectangular cell (see Fig. 2a)
C_m	heat capacity of metal
E	average electric field in solution or average temperature gradient in medium
I	total current in unit cell
I_F	faradaic current in unit cell
I_S	by-pass current in solution in unit cell
i_c	cathodic limiting current density
j	current density
n	normal distance from the electrode surface
r, θ	polar coordinates
r_0	radius of cylindrical electrode
S	surface area of electrode
t	time
V	cell voltage
V_0	threshold voltage or theoretical decomposition voltage
$v(x, y, t)$	hypothetical temperature which, for $t = \infty$, corresponds to $\phi_s(x, y)$
$v_m(t)$	hypothetical temperature which, for $t = \infty$, corresponds to ϕ_m
w	complex number defined in Fig. 2c
x, y	Cartesian coordinates
z	complex number defined in Fig. 2a
α	thermal diffusivity
ζ	complex number defined in Fig. 2b
η_c	cathodic overpotential
κ	electric conductivity of solution or thermal conductivity of medium
ϕ_m	potential of metal
$\phi_s(x, y)$	potential of solution

Subscripts

i, j, k	ordinal numbers of division of x, y, t

1. Introduction

Theoretical analysis of the current distribution in electrolytic cells has been one of the major subjects in electrochemical engineering. Potential and current distributions are also important in operation of batteries and fuel cells and in the prediction and prevention of metallic corrosion. Most of the theoretical work so far reported is concerned with the solution of the Laplace equation using analytical and numerical methods [1–14].

We have been interested in the potential and current distributions in packed bipolar cells in which conducting particles behave as bipolar electrodes [15–19]. In this type of cell it is difficult to solve the Laplace equation to obtain the potential distribution in solution, since boundary conditions at the surface of a bipolar electrode cannot be formulated explicitly. Thus the anodic and cathodic areas and the current density on the bipolar electrode are not prescribed, but must be obtained as the result of calculation.

In an effort to deal with such a problem, we proposed to use the differential equation of non-steady-state heat conduction, instead of the Laplace equation, and found that the method is useful and also applicable to other systems [20, 21]. The present paper

0021-891X/89 $03.00 + .12

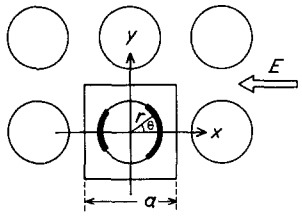

Fig. 1. Two-dimensional model of a bipolar electrode.

describes the general idea of the method and some calculation results. For simplicity only two-dimensional problems have been considered.

2. Theory

In order to describe the principle of calculation we consider a special example, that is, a two-dimensional model of a packed bipolar cell [18], since extension of the method to other systems is straightforward. Let us assume that conducting cylinders are arranged parallel to each other with a square lattice configuration in an electrolytic solution, as shown in Fig. 1. If there is no concentration gradient of ionic species in the solution, the potential of solution $\phi_s(x, y)$ satisfies the Laplace equation [5]:

$$\frac{\partial^2 \phi_s(x, y)}{\partial x^2} + \frac{\partial^2 \phi_s(x, y)}{\partial y^2} = 0 \qquad (1)$$

When a sufficiently large field is applied in the solution, each cylinder becomes a bipolar electrode; anodic and cathodic reactions take place on the opposite sides of each cylinder. Then we need to know the potential distribution in a unit cell indicated by the square in Fig. 1. Boundary conditions at the outer limit of the unit cell are written as

$$\left\{\frac{\partial \phi_s(x, y)}{\partial y}\right\}_{y=\pm a/2} = 0 \qquad (2)$$

$$\phi_s(a/2, y) = \phi_s(-a/2, y) + Ea \qquad (3)$$

where E is the average electric field in the solution. Since the anodic and cathodic current densities on the electrode surface are functions of the local potential difference between the metal and the solution, the following equation holds:

$$\kappa \left\{\frac{\partial \phi_s(x, y)}{\partial n}\right\}_{n=0} = f\{\phi_m - \phi_s(x, y)\} \qquad (4)$$

Here, n is the normal distance from the electrode surface, and κ is the electric conductivity of the solution. Since the total anodic and cathodic currents on the bipolar electrode must cancel each other, the equation

$$\int \kappa \left\{\frac{\partial \phi_s(x, y)}{\partial n}\right\}_{n=0} dS = 0 \qquad (5)$$

should hold, where dS is an infinitesimal area of the electrode surface and the integration is performed over the whole surface of the electrode. In principle the potential distribution can be obtained by solving Equation 1 under the limiting conditions of Equations 2–5. However, it is difficult to do so even by a numerical method.

Let us now consider a differential equation of heat conduction which describes the time-dependent temperature distribution in a uniform medium [22]:

$$\frac{\partial v(x, y, t)}{\partial t} = \alpha \left\{\frac{\partial^2 v(x, y, t)}{\partial x^2} + \frac{\partial^2 v(x, y, t)}{\partial y^2}\right\} \qquad (6)$$

Here, t is the time, $v(x, y, t)$ is the temperature as a function of x, y and t, and α is the thermal diffusivity of the medium. At steady state ($\partial v(x, y, t)/\partial t = 0$), Equation 6 becomes the Laplace equation for the temperature. Therefore, if $v(x, y, t)$ satisfies appropriate limiting conditions corresponding to Equations 2–5, the steady-state distribution of $v(x, y, t)$ can simulate the distribution of the potential $\phi_s(x, y)$ described above. The electrode is then regarded as a metal with infinite thermal conductivity (perfect conductor). The boundary conditions corresponding to Equations 2–4 are written as

$$\left\{\frac{\partial v(x, y, t)}{\partial y}\right\}_{y=\pm a/2} = 0 \qquad (7)$$

$$v(a/2, y, t) = v(-a/2, y, t) + Ea \qquad (8)$$

$$\kappa \left\{\frac{\partial v(x, y, t)}{\partial n}\right\}_{n=0} = f\{v_m(t) - v(x, y, t)\} \qquad (9)$$

where $v_m(t)$ is the temperature of the metal. In this case E is regarded as the average temperature gradient, and κ as the thermal conductivity of the medium. The limiting condition corresponding to Equation 5 is the equation representing the heat balance on the metal. Thus,

$$C_m \frac{dv_m(t)}{dt} = \int \kappa \left\{\frac{\partial v(x, y, t)}{\partial n}\right\}_{n=0} dS \qquad (10)$$

where C_m is the heat capacity of the metal. The integral on the right hand side of Equation 10 is the total heat flux into the metal, which should become zero at steady state ($dv_m(t)/dt = 0$), representing Equation 5. When the hypothetical quantities $v(x, y, t)$ and $v_m(t)$, according to Equations 6–10, converge at steady state, they are regarded as $\phi_s(x, y)$ and ϕ_m, respectively.

In the case of conventional cells for which the anode and the cathode are located separately and a constant voltage is applied to them we can assign constant values of v_m to the anode and the cathode. If a constant current is applied, the v_m values of the anode and the cathode are expressed by separate equations which are similar to Equation 10, but contain the constant current term.

3. Calculation

The finite difference approximation was used in the numerical calculations. When the variables x, y and t are digitized with increments Δx, Δy and Δt, a finite

difference expression of Equation 6 is derived as

$$\frac{v_{i,j,k+1} - v_{i,j,k}}{\Delta t} = \alpha \left(\frac{v_{i+1,j,k} - 2v_{i,j,k} + v_{i-1,j,k}}{\Delta x^2} + \frac{v_{i,j+1,k} - 2v_{i,j,k} + v_{i,j-1,k}}{\Delta y^2} \right) \quad (11)$$

where i, j and k are ordinal numbers corresponding to x, y and t, respectively. From Equation 11, $v_{i,j,k+1}$ is given by

$$v_{i,j,k+1} = v_{i,j,k} + \frac{\alpha \Delta t}{\Delta x^2} (v_{i+1,j,k} - 2v_{i,j,k} + v_{i-1,j,k}) + \frac{\alpha \Delta t}{\Delta y^2} (v_{i,j+1,k} - 2v_{i,j,k} + v_{i,j-1,k}) \quad (12)$$

The boundary conditions are also written in the form of difference equations. Equation 12, together with appropriate boundary conditions, enables us to calculate the v and v_m values at the time step k + 1 from the v and v_m values at the time step k. Calculation was continued until the rate of change in v values at some selected points became smaller than a certain level (0.01% for one time step). Convergence was confirmed by a few calculations starting from different initial conditions. In the case of a two-dimensional model of a packed bipolar cell, polar coordinates (r, θ) were adopted instead of Cartesian coordinates (see Fig. 1), and the relevant difference equation was used.

Potential maps (equipotential lines) were drawn by interpolating ϕ_s between lattice points. Current lines were obtained by making contours of the stream function which was calculated from ϕ_s values at lattice points. Current density at the electrode surface was calculated by

$$j = \kappa \left\{ \frac{\partial \phi_s(x, y)}{\partial n} \right\}_{n=0} \quad (13)$$

For calculation and display of results an NEC Model PC-9801F personal computer was used.

All the quantities are expressed in the dimensionless form, since any units can be used as long as they are consistent in the unit system.

4. Results and discussion

The primary potential and current distributions have been calculated as described above in a rectangular cell with an anode and a cathode of different sizes. Since the method of conformal mapping can also be applied in this case, we can test the validity of the numerical calculation. Figure 2a shows the geometry (top view) of the cell considered. The ratio of the cell width to the interelectrode distance is 2:1, and the ratio of the anode to cathode width is also 2:1. The cell walls other than the electrodes are insulators. Since the cell geometry is symmetrical with respect to the y axis, only a half of the cell (the square ABCDE) need be considered. The half cell width (AC) and the interelectrode distance (AE) were divided by 11 and 12 × 12 lattice points were located at intersections of the dividing lines and on the boundaries (electrodes and insulating walls). The odd number (11) was adopted for the division in order to avoid the edge of the cathode (singular point) as a lattice point. Values of $v_{i,j,k}$ were calculated stepwise, and it was found that they converged toward a steady state. Figure 3 shows equipotential lines and current lines thus obtained.

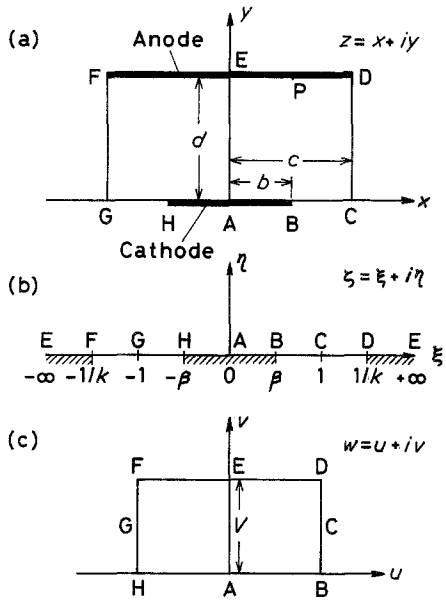

Fig. 2. Geometry of a rectangular cell (a) and corresponding figures in the ζ plane (b) and the w plane (c).

The primary potential distribution in a rectangular cell can also be obtained by the method of conformal mapping [3, 12, 22]. Fletcher Moulton first solved the problems of current flow in rectangular conductors [23]. Application of the Schwarz–Christoffel theorem to the present system leads to an analytical solution involving the elliptic integral of the first kind, which can be calculated numerically by Simpson's method (see Appendix). The solid lines in Fig. 4 show the current density distributions at the anode and the cathode obtained by the conformal mapping method,

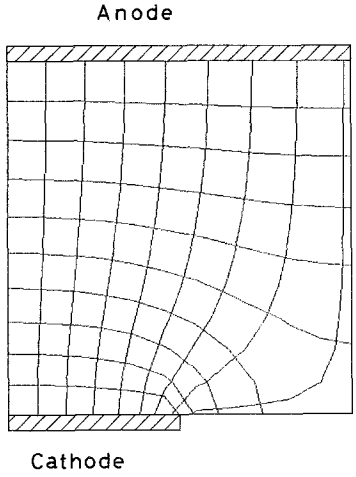

Fig. 3. Primary potential and current distributions in the rectangular cell. Cell and electrode sizes, $b = 0.5$, $c = 1$, $d = 1$; $\kappa = 1$; ϕ_s(anode) − ϕ_s(cathode) = 1; $I = 0.82$ (calculated). Equipotential lines are drawn at intervals of a tenth of the unit voltage. The separation between adjacent current lines corresponds to a tenth of the unit current.

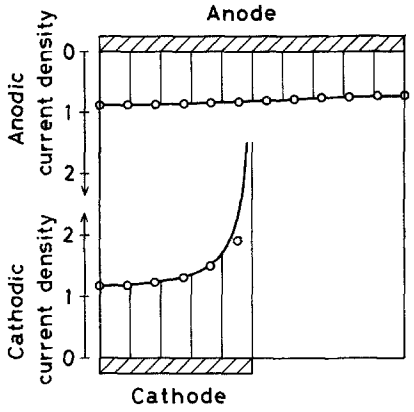

Fig. 4. Current densities at the anode and the cathode obtained by the numerical calculation (circles) and by the conformal mapping method (solid lines).

whereas the circles indicate the results of the numerical calculation by means of heat transfer equations. A good agreement is seen except near the edge of the cathode (point B) where the current density approaches infinity.

Figure 5 shows an example of the secondary potential and current distributions in the same cell. It is assumed that the overpotential at the anode is zero and the overpotential at the cathode is a linear function of the local current density; that is, the function in Equation 4 is expressed as

$$f(\phi_m - \phi_s(x, y)) = \phi_m - \phi_s(x, y) \qquad (14)$$

Calculation has been performed under the condition of constant current where the anode and the cathode are regarded as a source and a sink, respectively, of constant flow of heat which corresponds to the same current as in the previous calculation of primary distribution. It is noted that equipotential surfaces cross the cathode surface and that concentration of current lines at the edge of the cathode (point B) is reduced appreciably.

We have calculated the potential distribution in the two-dimensional model of a bipolar electrode shown in Fig. 1. Instead of Equation 11, the difference equation based on polar coordinates was used, and r

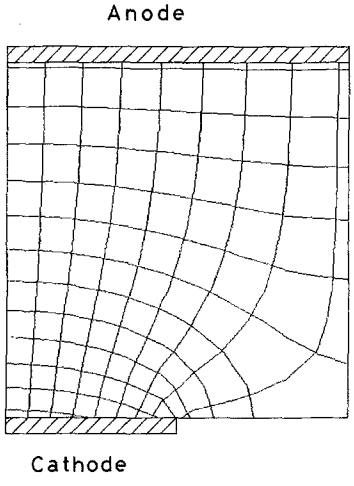

Fig. 5. Secondary potential and current distributions in the rectangular cell. $d\eta_c/dj = 1$; $I = 0.82$ (assumed). Otherwise see the caption of Fig. 3.

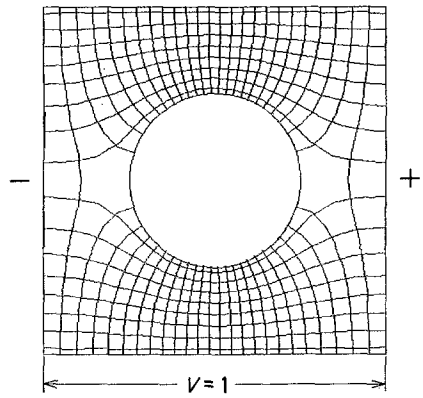

Fig. 6. Potential and current distributions around the bipolar electrode with no reactions occurring. $a = 2$; $r_0 = 0.5$; $E = 0.5$; $\kappa = 1$. $I_F = 0$ (calculated); $I_S = 0.35$ (calculated). Equipotential lines are drawn at intervals of a twenty-fifth of the unit voltage. The separation between adjacent current lines corresponds to a twenty-fifth of the unit current.

and θ were digitized with $\Delta r = a/20$ and $\Delta\theta = 10°$, respectively. Since the unit cell is symmetrical with respect to the x-axis, calculation was performed only in the upper half of the unit cell. Figure 6 shows the potential and current lines in the unit cell when no reaction occurs on the electrode. This situation arises when the applied field is relatively low. The electrode behaves as an insulator, and all the current flows through the solution. Figure 7 shows the other extreme in which the anodic and cathodic reactions are the same but proceed in the opposite directions with no overpotential. The potential distribution is compared to the temperature distribution in a uniform medium in which a perfect heat conductor is placed.

The secondary potential and current distributions have been calculated in the case where the anodic and cathodic reactions are characterized by Fig. 8. Thus the overpotential at the anode is zero, while the cathodic current–potential relationship is modelled by a step function. Figure 9 shows the potential and current lines obtained. It is noted that the cathode area is larger than the anode area under the present conditions. By repeating similar calculations for different values of applied voltage, we can obtain cell characteristics (such as the effective electrode area and

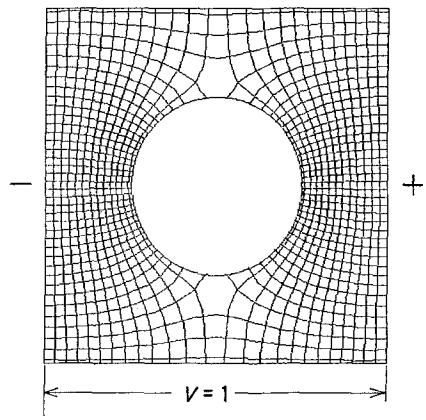

Fig. 7. Potential and current distributions around the bipolar electrode with reactions of $V_0 = 0$ and with no overpotentials. See the captions of Fig. 6. $I_F = 0.55$ (calculated); $I_S = 0.13$ (calculated).

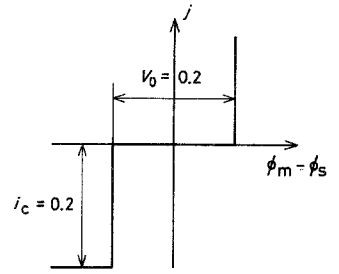

Fig. 8. A model of current–potential relationship. $V_c = 0.2$; $i_c = 0.2$.

energy efficiency) as functions of the applied voltage, as described previously [18, 19].

Various types of current–potential relationships, including the Tafel and Butler–Volmer types, can be treated similarly by using appropriate functions in Equation 4. The present method is applicable not only to conventional types of electrochemical cells (electrolysers and batteries) but also to more complicated systems such as corrosion cells in which the anodic and cathodic areas are not separated [21]. Furthermore it may be possible to calculate the tertiary current distribution involving diffusion and convection by solving Equation 6 and relevant mass transfer equations simultaneously.

Appendix

When we transform the inside of the rectangle ABCDEFGH in the z plane (Fig. 2a) into the upper half of the ζ plane (Fig. 2b), the Schwarz–Christoffel theorem gives the equation

$$\frac{dz}{d\zeta} = \frac{A}{\sqrt{(1-\zeta^2)(1-k^2\zeta^2)}} \quad (0 < k < 1) \qquad (A1)$$

where A is a constant which must satisfy the conditions below. Since $\zeta = 0$ at $z = 0$,

$$z = A\int_0^{\zeta} \frac{d\zeta}{\sqrt{(1-\zeta^2)(1-k^2\zeta^2)}} \qquad (A2)$$

The integral is the elliptic integral of the first kind with the modulus k and can be rewritten by replacing $\zeta = \sin\theta$ as

$$\int_0^{\theta} \frac{d\theta}{\sqrt{1-k^2\sin^2\theta}} \qquad (A3)$$

The latter form is suitable for the numerical calculation by Simpson's method, since the integrand is always finite for $0 \leqq \theta \leqq \pi/2$ $(0 \leqq \zeta \leqq 1)$. Integration of Equation A1 from the point A ($z = 0$) to the point C ($z = c$) yields

$$c = A\int_0^1 \frac{d\zeta}{\sqrt{(1-\zeta^2)(1-k^2\zeta^2)}} = AK \qquad (A4)$$

where K is the complete elliptic integral of the first kind. Integration of Equation A1 from the point C ($z = c$) to the point D ($z = c + id$) yields

$$id = A\int_1^{1/k} \frac{d\zeta}{\sqrt{(1-\zeta^2)(1-k^2\zeta^2)}} = iA\int_0^1 \frac{d\zeta}{\sqrt{(1-\zeta^2)\{1-(1-k^2)\zeta^2\}}} = iAK' \qquad (A5)$$

where K' is the complete elliptic integral of the first kind with the complementary modulus $(1-k^2)^{1/2}$. From Equations A4 and A5 the equation

$$K/K' = c/d \qquad (A6)$$

should hold. Since both K and K' are functions of k, we can determine k, K and K' from Equation A6. In the above calculations we can obtain numerical values of the complete elliptic integral either by Simpson's method or by a polynominal approximation for the integral [24]. Then A is obtained from Equation A4, and ζ can be calculated from Equation A2

$$\zeta = \mathrm{sn}(z/A) \qquad (A7)$$

Here, $\mathrm{sn}(z/A)$ is Jacobi's elliptic function. Since $\zeta = \beta$ at the point B ($z = b$), β is obtained as $\beta = \mathrm{sn}(b/A)$.

Now we transform the upper half of the ζ plane into the inside of the rectangle ABCDEFGH in the w plane (Fig. 2c). The Schwarz–Christoffel theorem yields

$$\frac{dw}{d\zeta} = \frac{B}{\sqrt{(\beta^2-\zeta^2)(1-k^2\zeta^2)}} \qquad (A8)$$

which is integrated from the point B to the point D giving the equation

$$V = B\int_0^1 \frac{d\zeta}{\sqrt{(1-\zeta^2)\{1-(1-k^2\beta^2)\zeta^2\}}} \qquad (A9)$$

Since k, β and V are the known quantities, B can be calculated. For $b = 0.5$, $c = 1$ and $d = 1$, the following values are obtained: $k = 0.707$, $\beta = 0.765$, $A = 0.539$ and $\beta = 0.479$.

Current density is expressed by

$$j = \kappa\left|\frac{dw}{dz}\right| = \kappa\left|\frac{dw}{d\zeta}\right|\Big/\left|\frac{dz}{d\zeta}\right| = \kappa\frac{B}{A}\left|\sqrt{\frac{\zeta^2-1}{\zeta^2-\beta^2}}\right| \qquad (A10)$$

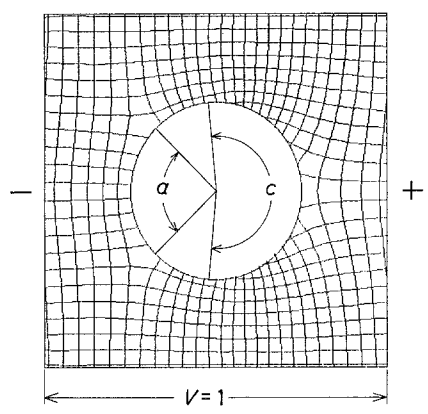

Fig. 9. Potential and current distributions around the bipolar electode with no overpotential at the anode and with the limiting current behaviour of the cathode. See the caption of Fig. 6. a, anode area; c, cathode area. $I_F = 0.16$ (calculated); $I_S = 0.29$ (calculated).

Integration of Equation A1 from the point P ($z = x + id$) on the segment DE to the point E ($z = id$) yields

$$x = A\int_{\zeta}^{+\infty} \frac{d\zeta}{\sqrt{(1-\zeta^2)(1-k^2\zeta^2)}} = A\int_{0}^{1/k\zeta} \frac{d\zeta}{\sqrt{(1-\zeta^2)(1-k^2\zeta^2)}} \quad \text{(A11)}$$

The current density at the anode can be calculated as a function of x, since j and x are both functions of ζ, as given by Equations A10 and A11. Similarly, the current density at the cathode can be obtained from Equations A10 and A2 with $z = x$.

References

[1] C. Wagner, *J. Electrochem. Soc.* **98** (1951) 116.
[2] C. W. Tobias and R. Wijsman, *J. Electrochem Soc.* **100** (1953) 459.
[3] F. Hine, S. Yoshizawa and S. Okada, *J. Electrochem. Soc.* **103** (1956) 186.
[4] J. A. Klingert, S. Lynn and C. W. Tobias, *Electrochim. Acta* **9** (1964) 297.
[5] J. Newman, 'Electrochemical Systems', Prentice Hall, Engelwood Cliffs, NJ (1973).
[6] S. Yoshizawa (editor), 'Denki Kagaku', Vol. 3, Kyoritsu-shuppan, Tokyo (1974).
[7] R. Alkire, T. Bergh and R. L. Sani, *J. Electrochem. Soc.* **125** (1978) 1981.
[8] M. Takahashi and N. Masuko, 'Kogyodenkai no Kagaku', Agune, Tokyo (1979).
[9] N. Ibl, 'Comprehensive Treatise of Electrochemistry', Vol. 6, Plenum Press, New York (1983) pp. 239–315.
[10] Y. Nishiki, K. Aoki, K. Tokuda and H. Matsuda, *J. Appl. Electrochem.* **14** (1984) 653.
[11] F. Hine, 'Electrode Processes and Electrochemical Engineering', Plenum Press, New York (1985).
[12] H. Kawamoto, *Denki Kagaku* **53** (1985) 98.
[13] H. Shih and H. W. Pickering, *J. Electrochem. Soc.* **134** (1987) 551.
[14] E. C. Dimpault-Darcy and R. E. White, *J. Electrochem. Soc.* **135** (1988) 656.
[15] S. Yoshizawa, Y. Mayazaki and A. Katagiri, *Nippon Kagaku Kaishi* (1977) 19.
[16] S. Yoshimura, A. Katagiri and S. Yoshizawa, *Nippon Kagaku Kaishi* (1978) 1144.
[17] Y. Miyazaki, A. Katagiri, S. Yoshizawa and Z. Takehara, *Mem. Fac. Eng. Kyoto Univ.* **49** (1987) 162.
[18] Y. Miyazaki, A. Katagiri and S. Yoshizawa, *J. Appl. Electrochem.* **17** (1987) 113.
[19] Y. Miyazaki, A. Katagiri and S. Yoshizawa, *J. Appl. Electrochem.* **17** (1987) 877.
[20] A. Katagiri and Y. Miyazaki, Abstract No. G324, presented at the 54th Meeting of the Electrochemical Society of Japan, 5–7 April 1987, Osaka.
[21] A. Katagiri, Abstract No. D105, presented at the 55th Meeting of the Electrochemical Society of Japan, 5–7 April 1988, Tokyo.
[22] H. S. Carslaw and J. C. Jaeger, 'Conduction of Heat in Solids', Oxford University Press, London (1959).
[23] H. Fletcher Moulton, *Proc. London Math. Soc., Ser. 2* **3** (1905) 104.
[24] M. Abramowitz and I. A. Stegun, 'Handbook of Mathematical Functions', Dover, New York (1970) p. 591.